Research paper

Patterns and variability in seedling carbon assimilation: implications for tree recruitment under climate change

Drew M.P. Peltier[1,3] and Inés Ibáñez[2]

[1]School of Life Sciences, Arizona State University, Tempe, AZ, USA; [2]School of Natural Resources and Environment, University of Michigan, Ann Arbor, MI, USA; [3]Corresponding author (dpeltier@asu.edu)

Predicting future forests' structure and functioning is a critical goal for ecologists, thus information on seedling recruitment will be crucial in determining the composition and structure of future forest ecosystems. In particular, seedlings' photosynthetic response to a changing environment will be a key component determining whether particular species establish enough individuals to maintain populations, as growth is a major determinant of survival. We quantified photosynthetic responses of sugar maple (*Acer saccharum* Marsh.), pignut hickory (*Carya glabra* Mill.), northern red oak (*Quercus rubra* L.) and eastern black oak (*Quercus velutina* Lam.) seedlings to environmental conditions including light habitat, temperature, soil moisture and vapor pressure deficit (VPD) using extensive in situ gas exchange measurements spanning an entire growing season. We estimated the parameters in a hierarchical Bayesian version of the Farquhar model of photosynthesis, additionally informed by soil moisture and VPD, and found that maximum Rubisco carboxylation (V_{cmax}) and electron transport (J_{max}) rates showed significant seasonal variation, but not the peaked patterns observed in studies of adult trees. Vapor pressure deficit and soil moisture limited J_{max} and V_{cmax} for all four species. Predictions indicate large declines in summer carbon assimilation rates under a 3 °C increase in mean annual temperature projected by climate models, while spring and fall assimilation rates may increase. Our model predicts decreases in summer assimilation rates in gap habitats with at least 90% probability, and with 20–99.9% probability in understory habitats depending on species. Predictions also show 70% probability of increases in fall and 52% probability in spring in understory habitats. All species were impacted, but our findings suggest that oak species may be favored in northeastern North America under projected increases in temperature due to superior assimilation rates under these conditions, though as growing seasons become longer, the effects of climate change on seedling photosynthesis may be complex.

Keywords: Bayesian, drought, photosynthetic parameters, seasonality, transplant.

Introduction

Under the current climatic trends, northeastern North American forests will be subjected to increased average temperatures, decreased average precipitation along with the altered timing of rainfall, increased environmental variability and an increased frequency of extreme events (IPCC 2007, 2013). In the long term, these trends are predicted to lead to future changes in tree species' distributional ranges (Iverson et al. 2008). But, in the short term, and at a given location, some species may be able to persist in the new environment, whereas others may experience increased mortality (Allen et al. 2010) or decreased recruitment success (Ibáñez et al. 2008). Despite the major implications of such disparate responses, we do not fully understand which outcome will be more likely for most species in North America. In order to predict the future state of these forests, we will need to make accurate predictions about tree population dynamics under projected environmental conditions. In particular, understanding how recruitment of new individuals is affected by changing conditions may confer the

most useful information, because this life stage will likely be the most affected by climate change (Ibáñez et al. 2009).

While adult trees may cope with variable and non-optimum conditions over decadal time scales, seedlings may not, as survivorship typically increases with age class (e.g., De Steven 1994). Tree seedlings exhibit very high mortality in comparison with adults, constituting a bottleneck on population growth (Harper 1977, Harcombe 1987). Seedlings cannot utilize resources from as large a volume of soil as adult trees due to their smaller size. They also lack comparable reserves to adults to cope with sustained periods of unfavorable conditions, which makes their survival more dependent upon their environment (e.g., Kobe et al. 1995, Gray and Spies 1997, Matthes and Larson 2006, Comita et al. 2009).

In order to survive and further recruit to larger size classes, seedlings need to assimilate some minimum level of carbon to maintain growth (Caspersen and Kobe 2001, Ibáñez and McCarthy-Neumann 2013), which they use for radial growth, maintenance respiration, fine root production and leaf formation (Mooney 1972), supporting mycorrhizal symbionts (Norton et al. 1990) and other functions. Photosynthetic rate is dependent on environmental conditions. The role of light in assimilation and growth is well established (Burkholder 1936, Johnston 1940, Farquhar et al. 1980, Quero et al. 2008). Low soil moisture results in stomatal closure to prevent desiccation, limiting CO_2 exchange (Havranek and Benecke 1978). Moreover, temperature modifies photosynthetic rates (Dillaway and Kruger 2014); however, the effects are more complex, as photosynthesis consists of multiple processes (electron transport and RUBP regeneration [J_{max}], Rubisco carboxylation [V_{cmax}], dark respiration [R_d] and photorespiration) all having different temperature dependencies (Caemmerer 2000). While photosynthetic rate may increase with temperature, so will dark respiration (Man and Lieffers 1997, Dreyer et al. 2001), though dark respiration has been shown to acclimate to sustained changes in temperature over time (Tjoelker et al. 2001, Rodríguez-Calcerrada et al. 2010) while photosynthesis may not (Liang et al. 2013).

Photosynthetic processes themselves are also highly variable, as a number of key photosynthetic parameters vary significantly across the growing season. Net photosynthetic capacity (at saturating light) peaked during early spring for five North American tree species (Augspurger et al. 2005). Somewhat in contrast, for 23 temperate tree species photosynthetic rates were found to peak around the summer solstice, or the maximum photoperiod (Bauerle et al. 2012). Similarly, Zhu et al. (2011) found that for a single tree species dark respiration (R_d) was highest and mesophyll conductance (g_m) was lowest in spring, representing a potential limitation to spring assimilation. Others have found peak dark respiration in mid-summer (Koniger et al. 2000). And Wilson et al. (2000) found slightly different peak times for maximum Rubisco carboxylation (V_{cmax}) and maximum electron transport rates (J_{max}) in mature Acer rubrum L., Acer saccharum Marsh.

and Nyssa sylvatica Marsh. trees. While leaf-level physiology is only one component of whole plant carbon balance, it is important to account for this variability across the growing season to accurately estimate seasonal carbon budgets of forest seedlings, and ultimately, their ability to acclimate to future climate.

Changing climate will influence these environmental variables in a number of ways. In the Great Lakes region (where our study took place), average annual precipitation is projected to increase along with temperature (IPCC 2013). However, increased summer temperature and increased variability in precipitation, with a higher frequency of extreme events (IPCC 2007), may lead to decreased soil moisture and increased vapor pressure deficits (VPD) on average. This could decrease seedlings' assimilation rates through more frequent stomatal limitation or increased total seasonal dark respiration, leading to decreased seasonal carbon assimilation. Finally, as the climate warms, many tree species will leaf out earlier or later in response to temperature cues, while other species may not be affected or even experience incomplete or asynchronous budburst in response to insufficient winter chilling (Morin et al. 2009, Laube et al. 2014). This could lead to longer growing seasons for some species as spring and fall become warmer (Menzel and Fabian 1999). As future responses to changing climate may differ among and within species, across ontogenetic stages (seedlings vs adults) or habitats (low vs high light levels), it is crucial that we understand the processes that determine seedling carbon budgets according to the environment to which they are exposed.

In order to better understand how environmental conditions affect seedling carbon assimilation and to investigate how different species may respond to these conditions in the future, we measured the photosynthetic rates of 78 tree seedlings from four species, across a single growing season from leaf out to senescence. Species vary in growth rates, drought tolerances, shade tolerances and successional statuses. These temporally extensive carbon assimilation data were analyzed to address the following questions: (i) How do commonly estimated photosynthetic parameters vary through the growing season among seedlings growing under field conditions? (ii) How are these parameters affected by environmental variables, specifically light availability, temperature, soil moisture and VPD within and among seasons? And, (iii) due to the direct and indirect effects of temperature on carbon assimilation, and the high certainty in predictions of future increases in mean temperature, we ask how might the photosynthetic assimilation rates of four important tree species be impacted under projected increases in temperature due to climate change?

Materials and methods

Study site

In the summer of 2012, we conducted gas exchange measurements of seedlings from several tree species (A. saccharum,

Carya glabra Mill., *Quercus rubra* L. and *Quercus velutina* Lam.; Table S1 available as Supplementary Data at *Tree Physiology* Online) of varying drought and shade tolerances and growth rates (Barnes and Wagner 2004) on 74 days between Julian days 121 and 297 at the E. S. George Reserve, Pinckney, MI, USA (~42°28′N, −84°00′W, ~280 m above sea level). The area is composed of reforested farmland, woodlots and pasture, with primarily oak–hickory forest growing on sandy loam to loamy sand soils. Average annual precipitation is 762 mm spread throughout the year with mean monthly temperatures ranging from −5.5 °C in January to 22 °C in July and with an average growing season length of 145 days. We worked at two sites separated by <1 km; Site 1 is representative of a sugar maple-mixed Oak forest (*A. saccharum*, *Q. rubra*, *Q. velutina* and *Quercus alba* L.), and Site 2 is a black oak–hickory forest (*Q. velutina* and *C. glabra*). These sites were selected because they represent two major local vegetation types and contain some of the most dominant species in the region. The 2012 summer was characterized by high drought and heat indices with summer precipitation being almost half of average (Andresen 2012) with only ~214 mm falling between May and September (NOAA National Climatic Data Center 2012).

In order to have a representative sample of different light conditions (determined via hemispheric canopy photos), we measured seedling photosynthetic rates in forest research plots (5 × 5 m) established across natural light habitats: understory (or canopy) (mean ± SD: ~10.4 ± 0.01% full sunlight at Site 1 and 21.0 ± 0.03% at Site 2) and gap (49.1 ± 0.1% at Site 1, 84.9 ± 0.1% at Site 2). Full sunlight was ~2200 μmol m^{-2} s^{-1} photosynthetically active radiation (PAR). Greenhouse-raised first-year seedlings of each of the four study species were tagged and transplanted (bare root) into several plots in the early summer of 2009 and 2010 (see Ibáñez and McCarthy-Neumann 2013 for growing information). Forty-seven transplanted seedlings across five plots were used in this study. Due to low seedling survival in the understory habitat at Site 1, we used an additional understory plot at this site to obtain enough replicates (Site 1: two understory plots and one gap plot; Site 2: one understory plot and one gap plot). In addition to the transplanted seedlings, 31 natural seedlings (3–7 years old, aged using terminal bud scars) were located within or adjacent to plots and added to the study in July, for a total of 78 seedlings distributed across sites, light habitats and species. Due to extremely low survival of the transplants, there were no transplanted *A. saccharum* seedlings in gap habitats, therefore measurements of *A. saccharum* in gaps only began in July with the addition of the natural seedlings.

Data collection

One environmental microstation (HOBOware, Onset Computer Corp., Bourne, MA, USA) was established at each site in the understory habitat, and soil moisture, air temperature and PAR were measured every 60 min throughout the year. Some of the temperature data for the spring season at Site 1 were lost due to equipment malfunction; however, enough remained for accurate representation of spring temperature, and the mean and standard deviation agreed well with the data from Site 2.

For a finer scale calibration of soil moisture measurements, volumetric water content (VWC) was recorded with a soil moisture probe (Fieldscout—TDR 300 Soil Moisture Meter, Spectrum Technologies, Plainfield, IL, USA) at each corner of the plots, at four points immediately adjacent to each seedling and at four points immediately surrounding the microstation probes. These measurements were conducted four to 10 times per plot over the season, beginning in July and ending in mid-October (~Julian day 297), wherein the date and time of measurement to the nearest 30 min were recorded. We used this combination of temporally extensive measurements with the data logger and spatially extensive manual measurements with the probe to recreate the soil moisture environment each seedling was exposed to during the photosynthetic measurements (see Appendix S1 available as Supplementary Data at *Tree Physiology* Online).

Hemispheric canopy photos (Rich 1990) were taken at the corner of each plot and directly above each natural seedling after full overstory had developed. Photos were analyzed with the Hemiview hemispheric image analysis system (Dynamax, Inc., Houston, TX, USA) and the global site factor (proportion of incident global solar flux) was calculated for each plot and each natural seedling.

Gas exchange

Measurements were taken at steady state (and we did not directly account for dynamic conditions, such as sunflecks) across a range of temperatures, soil moistures and times of day in an attempt to capture a large range of variability under environmental conditions. Gas exchange measurements were collected with two LI-6400 Portable Photosynthesis Systems equipped with CO$_2$ mixer assemblies, LI-02B LED red/blue light sources and LI-06 PAR sensors (Li-COR Biosciences, Lincoln, NE, USA). Light response (A–Q) curves were taken at ambient humidity and temperature at CO$_2$ concentrations of 390 ppm at 11 descending light levels (1500, 1000, 750, 500, 250, 125, 60, 30, 20, 10 and 0 μmol m^{-2} s^{-1}). Measured PAR at the LI-6400 sensor head in gap plots often exceeded 1500 μmol m^{-2} s^{-1} on sunny days and values >2000 μmol m^{-2} s^{-1} were observed. Photosynthetically active radiation in understory plots was lower (Figure S1 available as Supplementary Data at *Tree Physiology* Online), but frequently exceeded 1200 μmol m^{-2} s^{-1} in sunflecks and fluxes as high as 1800 μmol m^{-2} s^{-1} were observed. For this reason we chose to use the same light levels in both understory and gap plots. CO$_2$ response curves (A–C$_i$) were taken at saturating light (1500 μmol m^{-2} s^{-1}) at either nine CO$_2$ concentrations (in order: 400, 300, 200, 100, 50, 400, 400, 600 and 800 ppm) or, beginning on Julian day 202, to improve estimates of J$_{max}$, 11 CO$_2$ concentrations (in order: 400, 300, 200, 100, 50, 400, 400, 600, 800, 1000 and 1500 ppm), as it was observed

that some curves were not saturating at high C_i. A–C_i curves were performed immediately after A–Q curves (in most cases), after allowing seedlings to reacclimate to saturating light for at least 3 min, or until the assimilation rate was close to the maximum rate measured during the previous A–Q curve. These protocols were performed on seedlings of the four species in each plot no less than five times, unless the seedling died (<5%, three seedlings), across the growing season from early May to mid-October. While the spring of 2012 was very warm and leaf out took place earlier than normal, no seedlings showed any signs of frost damage. Since we did not have enough measurements to treat the date of measurement as a continuous variable (e.g., Julian day of measurement), we chose to bin the data into three seasons, based on natural breaks, defined as Julian days 121–145 (spring), 172–209 (summer) and 225–297 (fall). Observations that were clearly the result of mechanical error or non-equilibrium measurement (i.e., negative or extremely high intercellular CO_2 concentrations) were discarded from analysis. The LI-6400 also recorded simultaneous leaf and ambient temperatures, relative humidity, pressure, VPD and ambient PAR (μmol m^{-2} s^{-1}). For leaves <6 cm^2 gasket area (<5% of the measurements), a tracing of the leaf was made and dated at the time of measurement. Photographs of tracings were taken next to a ruler, and area of leaf tracings was subsequently estimated using ImageJ software (Schneider et al. 2012). Assimilation data were subsequently recomputed with the correct leaf areas in the LI-SIM software (Li-COR Biosciences).

Analysis

We analyzed our data following the Patrick et al. (2009) approach, utilizing the model code available in the Supplementary Data at *Tree Physiology* Online. In this model, the parameters of the Farquhar model of C3 photosynthesis (Farquhar et al. 1980) are estimated in a hierarchical Bayesian framework. Patrick et al. (2009) modified the basic Farquhar model to incorporate light dependency of potential electron transport according to Farquhar and Wong (1984) and mesophyll conductance according to Caemmerer and Evans (1991), Caemmerer (2000) and Niinemets et al. (2009). We simplified their model structure, while including linear relationships with additional explanatory variables (soil moisture and VPD) and allowing seasonal variation in a subset of photosynthetic parameters (description below). It should be noted that we did not incorporate an explicit stomatal conductance model, but opted to modify the estimation of certain parameters with a semi-mechanistic statistical model (see Eq. [6]). This allowed us to model both stomatal and non-stomatal effects of soil moisture and VPD on assimilation without over-complicating the model. Data and parameter abbreviations, definitions, units, sources, functions and prior distributions are given in Table 1.

The observed assimilation rate, A_{obs}, at a specific light level, Q, and intracellular CO_2 concentration, C_i, for a particular observation, i, was modeled with a Normal likelihood with mean assimilation rate μA_i and variance σ^2:

$$A_{obs_i} \sim Normal(\mu A_i, \sigma^2)$$

Depending on the transitional concentration of CO_2 (C_{crit}), the assimilation rate μA is defined as the minimum of Rubisco carboxylation-limited ($\mu A = Av$ if $C_i < C_{crit}$) or RUBP-regeneration-limited ($\mu A = Aj$ if $C_i > C_{crit}$) rates of assimilation. We do not include TPU-limited photosynthesis in the model, as this has been shown to be rarely encountered under natural conditions (Dubois et al. 2007, Niinemets et al. 2009). For each observation i in curve c, the assimilation rate is estimated as:

$$Av_i = \frac{-b1_i + \sqrt{b1_i^2 - 4 \times a1_i \times c1_i}}{2 \times a1_i} \quad (1)$$

where

$$a1_i = -\frac{1}{g_{m_c}} \quad (1a)$$

$$b1_i = \frac{V_{cmax_c} - R_{d_c}}{g_{m_c}} + C_{i_i} + K_{c_c}\left(\frac{1 + O_i}{K_{o_c}}\right) \quad (1b)$$

$$c1_i = R_{d_c}\left(C_{i_i} + K_{c_c}\left(\frac{1 + O_i}{K_{o_c}}\right)\right) - V_{cmax_c}(C_{i_i} - \Gamma^*_c) \quad (1c)$$

or as:

$$Aj_i = \frac{-b2_i + \sqrt{b2_i^2 - 4 \times a2_i \times c2_i}}{2 \times a2_i} \quad (2)$$

where

$$a2_i = -\frac{1}{g_{m_c}} \quad (2a)$$

$$b2_i = \frac{(J_i/4) - R_{d_c}}{g_{m_c}} + C_{i_i} + 2\Gamma^*_c \quad (2b)$$

$$c2_i = R_{d_c}(C_{i_i} + 2\Gamma^*_c) - \frac{J_i}{4}(C_{i_i} - \Gamma^*_c) \quad (2c)$$

Light dependency is incorporated into the calculation of the electron transport rate (J_i) as:

$$J_i = \frac{Q2_i + J_{max_c} - \sqrt{(Q2_i + J_{max_c})^2 - 4 \times \theta_{season(c),plant(c)} \times Q2_i \times J_{max_c}}}{2 \times \theta_{season(c),plant(c)}} \quad (3)$$

$$Q2_i = \frac{Q_i \times \alpha(1 - f)}{2} \quad (4)$$

Table 1. Model parameters used, abbreviations and definitions, and the source (observed data), values used (reported in the literature) or the prior distribution or equation (Eq) used for their estimation.

Abbreviation	Definition	Value, distribution, equation
σ	Model standard deviation	$U(0,5)$
Av_i	Rubisco carboxylation-limited rate of CO_2 assimilation (μmol m^{-2} s^{-1})	Eq. (1)
Aj_i	RUBP regeneration-limited rate of CO_2 assimilation (μmol m^{-2} s^{-1})	Eq. (2)
Alpha	PSII activity in bundle sheath	0.85[1]
$(C_{crit_c})C_i$	(Transitional) Intercellular CO_2 concentration (Pa)	$N(20,1.4)$[2], observed data
E_p	Activation energy for temperature responses of g_m, J_{max}, K_c, K_o, R_d, V_{cmax} or Γ^* (kJ mol^{-1})	$N(\mu = 49.6, 50.13, 70.37, 29.83,$ $63.90, 65.48$ or $26.84, \sigma^2 = 10)$[2]
f	Spectral light quality factor	0.15[3]
g_{m_c}, g_m25_c, μg_m25_s	Mesophyll conductance (μmol m^{-2} s^{-1})	Eq. (5), (7), $N(0,10) > 0$[4]
Γ^*_c, Γ^*25_c	CO_2 compensation point without dark respiration (μmol m^{-2} s^{-1})	Eqs (5), $N(3.86,1) > 0$[2]
(J_{max}), J_i $\alpha J_{max}25_{s,l,p}$ $\mu J_{max}25_{s,l}$	(Maximum) rate of electron transport (μmol m^{-2} s^{-1})	Eqs (6), (3), (10), $N(55,10^3) > 0$[5,6,7]
K_{c_c}, K_c25_c	Rubisco Michaelis–Menten constant for CO_2 (Pa)	Eq. (5), $N(27.348,10^3) > 0$[2]
K_{o_c}, K_o25_c	Rubisco Michaelis–Menten constant for CO_2 (kPa)	Eq. (5), $N(16582,10^4) > 0$[2]
O_i	Intercellular O_2 partial pressure (Pa)	
P_i	Pressure (Pa)	Observed data
Q_i $(Q2_i)$	Photosynthetically active radiation (μmol m^{-2} s^{-1}) (absorbed by PSII)	Observed data, Eq. (4)
R	Universal gas constant (J K^{-1} mol^{-1})	0.008314
R_{d_c}, R_d25_c, μR_d25_s	Daytime mitochondrial respiration rate (μmol m^{-2} s^{-1})	Eqs (5) and (8), $N(0,1) > 0$
T_i	Leaf temperature (K)	Observed data
$\theta_{s,p}$, $\mu\theta_s$	Empirical curvature factor	$N(\mu\theta_s, \theta\sigma_s)$, $N(0.7,10)(0–1)$[8]
$\theta\sigma^2_s$	Variance associated with $\mu\theta_s$	$U(0,100)$
V_{cmax_c} $\alpha V_{cmax}25_{s,l,p}$ $\mu V_{cmax}25_{s,l}$	Maximum rate of Rubsico carboxylation (μmol m^{-2} s^{-1})	Eqs (6) and (9), $N(25,10^3) > 0$[6,7,9]
$V\sigma^2_{s,l}$ $J\sigma^2_{s,l}$	Variance associated with $\alpha V_{cmax}25$ and $\alpha J_{max}25$ hyperparameters	$U(0,100)$
$\beta 1_s$, $\beta 2_l$	Soil moisture ($\beta 1_s$), VPD ($\beta 2_l$) coefficients for $V_{cmax}25$ and $J_{max}25$	$N(\mu = 0, \sigma^2 = 100, 10^3)$

Symbols μ, α and 25, indicate the means, hyperparameters, or temperature-adjusted (to 25 °C) values of a parameter. Subscripts indicate the level at which parameter is estimated: individual observation (i), curve (c), season (s), plant (p) and/or light habitat (l). Parameters without subscripts are estimated at the species level. Either Normal (N) or Uniform (U) prior distributions are used. Informative priors drawn from: [1]Caemmerer (2000); [2]Patrick et al. (2009); [3]Evans (1987); [4]Zhu et al. (2011); [5]Bethers et al. (2009); [6]DeLucia and Thomas (2000); [7]Wertin et al. (2011); [8]Evans (1989); [9]Aranda et al. (2005).

Parameters were estimated at the curve level, c, as there was a large amount of variability in observed photosynthetic rates among different measurements (Figure 1). For some of the parameters we used slightly informative prior distributions centered on literature values (Table 1). Certain parameters were truncated to prevent sampling of otherwise biologically meaningless values (such as negative dark respiration or a curvature factor >1; Table 1). One change we made to the basic process model is allowing the θ parameter, an empirical curvature factor for the light dependency Eq. (3), to vary across seasons (fixed effect) and among plants (random effects). We used an informative prior ($\mu\theta$ and $\theta\sigma$; Evans 1989) to estimate θ parameters of season–plant combinations for which we did not have data (some seedlings were added in the summer for which we do not have spring data).

$$\theta_{season(c),plant(c)} \sim Normal(\mu\theta_{season(c)}, \theta\sigma^2_{season(c)})$$

In addition, since A–C_i curves provide no information for the estimation of this parameter (as light is held constant in these curves) we presume that the θ parameter for each A–C_i curve is equal to the value of θ estimated for the light curve measured immediately before it, or in the absence of such data, the light curve measured closest to the date of the given A–C_i curve for the same plant (see 'Gas exchange').

As Rubisco carboxylation and oxygenation rates vary with temperature (Björkman et al. 1980), following Patrick et al. (2009) we used a linear Arrhenius function standardized to 25 °C to estimate mesophyll conductance, dark respiration, maximum Rubisco carboxylation rate, maximum electron transport rate, Michaelis–Menten constants for oxygenation and carboxylation and CO_2 photocompensation points (g_m, R_d, V_{cmax}, J_{max}, K_c, K_o and Γ^*) for each curve c. The same function was used for all seven of these parameters (p), where $p25_c$ is the value of parameter p_c at 25 °C for curve c and E_p is the activation energy for p_c:

$$p_c = p25_c \times e^{(E_p(T_i-298)/(298 \times R \times T_i))}. \qquad (5)$$

Data exploration suggested that both light and CO_2 saturated assimilation rates depended linearly on soil moisture (as VWC) and VPD, thus estimates of curve level V_{cmax} and J_{max} are also informed by these data (which was first 'mean-centered,' see
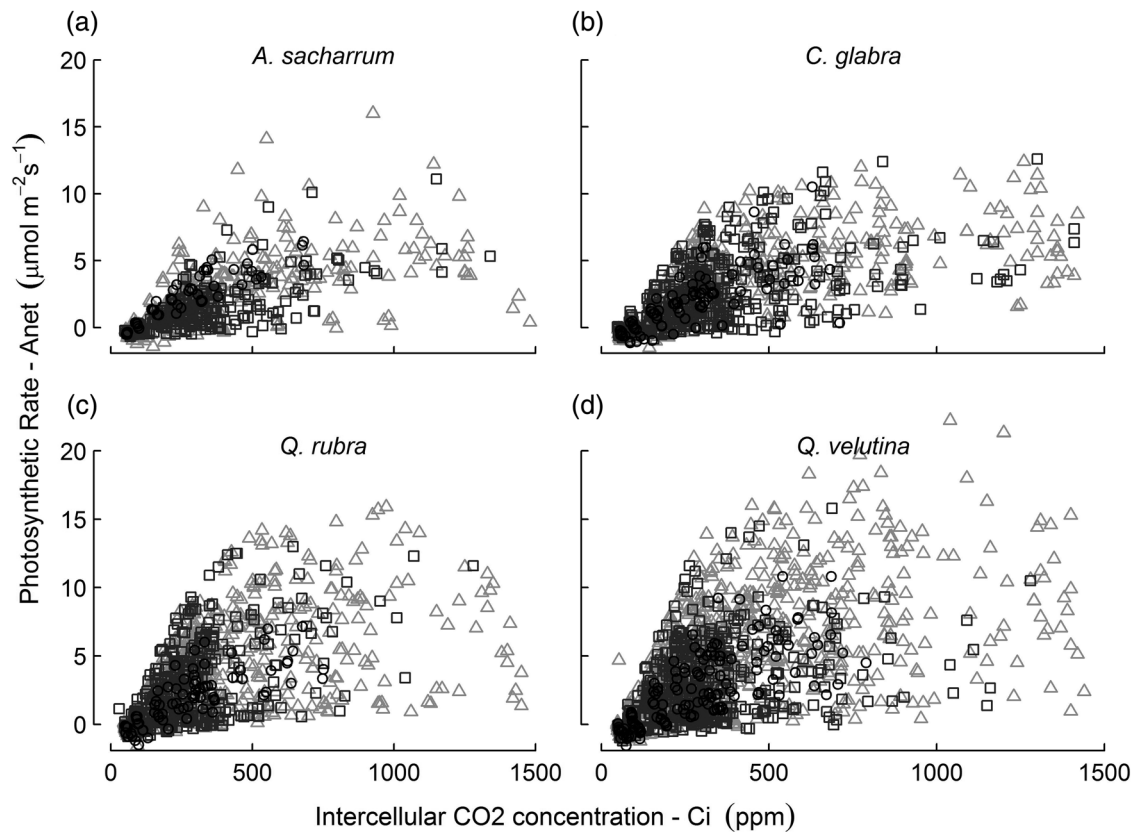
Figure 1. A–C_i curve datasets for spring (black circles), summer (dark gray squares) and fall (light gray triangles) showing observed variability in assimilation rates at a given C_i for (a) *A. saccharum*, (b) *C. glabra*, (c) *Q. rubra* and (d) *Q. velutina*. Curves were conducted at saturating light (~1500 μmol m^{-2} s^{-1}) and ambient humidity and temperature.

Appendix S1 available as Supplementary Data at *Tree Physiology* Online) in a semi-mechanistic model Eq. (6). Similar relationships were not observed with R_d or g_m, and attempts to include these data led to convergence issues, likely due to identifiability issues. This observed behavior is consistent with stomatal control of leaf intercellular CO_2 concentrations in response to internal abscisic acid (ABA) signaling from roots (Davies et al. 1980) and to increases in VPD (Oren et al. 1999). However, decreased leaf water potential under prolonged drought in field conditions may also decrease photosynthetic rates via its effect on the relative water content of cells (Björkman and Powles 1984, Kaiser 1987) and through decreased RUBP regeneration rates (Farquhar and Sharkey 1982, Tezara et al. 1999, Flexas and Medrano 2002). Since the LI-6400 calculates C_i from transpiration rates and the relative diffusivities of CO_2 and H_2O in air, much of the variation in assimilation due to changes in stomatal aperture is likely captured by this calculated variable (Sharkey et al. 1982). Therefore, in order to avoid further complication of the model, we chose not to incorporate a stomatal conductance model. The addition of soil moisture and VPD data further informs estimation of the assimilation rate by potentially capturing any non-stomatal effects of the water environment on J_{max} and V_{cmax}, and indirectly approximating the effects of these

variables on stomatal aperture, while keeping the model structure relatively simple. This means that the estimates for V_{cmax} and J_{max} are not equal to the 'true' values of these parameters in the absence of stomatal limitation. Rather, they represent 'effective' V_{cmax} and J_{max} under the mean environmental conditions observed in a given light habitat and season for that species.

Linear terms for soil moisture and VPD were incorporated into the Arrhenius temperature functions only for these two parameters (V_{cmax_c} and J_{max_c}). When we allowed the soil moisture relationship to vary seasonally (spring, summer and fall), it explained more variation than when we estimated a single value across the entire growing season. Similarly, the relationship with VPD (standardized, Appendix S1 available as Supplementary Data at *Tree Physiology* Online) appeared to differ by light habitat, and so was allowed to vary between habitats, canopy and gap.

$$p_c = p25_c \times e^{(E_p(T_i - 298)/(298 \times R \times T_i))} + \beta1_{season(c)} \text{ soil } mS_c + \beta2_{habitat(c)} \text{VPD}_c \quad (6)$$

The temperature-adjusted parameters g_m25_c and R_d25_c are essentially season-level parameters in order to capture any

seasonal changes in leaf biochemistry. Except for temperature, we could find no relationship between these two parameters and external environmental variables.

$$g_m 25_c = \mu g_m 25_{season(c)} \qquad (7)$$

$$R_d 25_c = \mu R_d 25_{season(c)} \qquad (8)$$

As seedlings' assimilation response to light may acclimate to different light levels, we included not only seasonal differences but also habitat differences (understory or gap) for $V_{cmax}25$ and $J_{max}25$. Because individual seedlings' assimilation rates were quite variable, we also allowed unique values for each season–plant–light habitat combination as

$$V_{cmax}25_c = \alpha V_{cmax}25_{season(c),habitat(c),plant(c)} \qquad (9)$$

$$J_{max}25_c = \alpha J_{max}25_{season(c),habitat(c),plant(c)} \qquad (10)$$

$$\alpha V_{cmax}25_{season(c),plant(c),habitat(c)}$$
$$\sim Normal(\mu V_{cmax}25_{season,habitat}, V\sigma^2_{season,habitat})$$

$$\alpha J_{max}25_{season(c),plant(c),habitat(c)}$$
$$\sim Normal(\mu J_{max}25_{season,habitat}, J\sigma^2_{season,habitat})$$

Prior distributions

We chose to use informative prior distributions for parameters which are not well estimated from our $A–Q$ and $A–C_i$ data, but are well documented in the literature, such as activation energies (E_p [Patrick et al. 2009]). Generally, we either used wider or the same variances as Patrick et al. (except for mesophyll conductance, which could not be reliably identified with wider variances). Since abundant literature is available on the values of certain photosynthetic parameters (for some plants), prior distributions were centered near literature values when available (Table 1).

Model implementation

We implemented the model using OpenBUGS software (Lunn et al. 2009). The final model was run with two chains for a burn-in of 50,000 iterations, after which samples were monitored to assess convergence of the chains using the Brooks–Gelman–Rubin test (Gelman and Rubin 1992). Chains were run after convergence to obtain at least 3000 independent samples for all parameters after thinning to remove within-chain autocorrelation. Model fit was evaluated using the R^2 between predicted and observed values.

Predicted assimilation response to projected temperature increases

To address Question (3), understanding how temperature increases due to climate change may affect seedlings' net assimilation rates, we used posterior estimates of model parameters to estimate net assimilation rates under current temperature averages and +3 °C scenarios, for each season and habitat. We chose to focus on the effects of temperature as this is a driving variable that influences VPD and biochemical reaction rates, while projections of precipitation are still uncertain at regional scales, and not well resolved to monthly timescales (IPCC 2013). And while mean annual precipitation is projected to increase, increased temperatures will likely drive increased evapotranspiration, potentially negating increases in average soil moisture availability (IPCC 2013). Due to this uncertainty, soil moisture values in mean and +3 °C scenarios were kept at observed summer 2012 averages for each season–habitat combination while VPD, which increases with temperature, was estimated in a VPD-temperature sub-model (see Appendix S2 and Table S2 available as Supplementary Data at *Tree Physiology* Online). Representative photosynthetic photon fluxes of 278 and 1076 µmol m^{-2} s^{-1}, calculated from the average global site factor in each light habitat (see 'Data collection'), were used for understory and open light habitats, respectively.

To evaluate the effect size of increased temperature, the effect of increased temperature on photosynthesis (ETP) was estimated by comparing the posterior probability density functions of predicted photosynthesis under current and elevated temperatures (Garrett and Zeger 2000). Comparisons are made within seasons at the average assimilation levels predicted at representative light levels (for understory and gap habitats) and seasonal mean soil moisture and VPD. The effect of increased temperature on photosynthesis is calculated as the ratio between the probability of achieving a photosynthetic rate as high or higher than the observed mean under current temperatures (the target rate) at elevated temperature and the probability of reaching the observed mean at current temperature, which is always equal to 0.5 (Figure S2 available as Supplementary Data at *Tree Physiology* Online). ETP > 1 indicates an increase in the probability of reaching the target rate and thus a positive effect of increasing temperature, and ETP < 1 indicates a decrease in the probability of reaching the target and thus a negative effect of a warmer environment.

Results

Environmental data

Soil VWC was highest in spring with midday means of 13.2 ± 2.0 and 13.9 ± 1.5% VWC for Sites 1 and 2, respectively. Soil moisture throughout summer was lower, with midday means of 3.1 ± 1.9

and $3.0 \pm 1.7\%$ VWC for Sites 1 and 2, respectively. Fall midday means were 5.3 ± 4.4 and $4.4 \pm 3.6\%$ VWC for Sites 1 and 2, respectively. Light levels at HOBO microstations in the canopy were uniformly low after canopy closure (~Julian day 140 and 160 for Sites 1 and 2, respectively), though PAR was higher and more variable at Site 2 (midday mean 38.7 ± 9.3 µmol m^{-2} s^{-1} for days 175–200) than at Site 1 (mean 17.5 ± 3.8 µmol m^{-2} s^{-1} for days 175–200), though many seedlings experienced higher average light levels. Mean midday temperatures for each season (spring, summer, fall) were 18.6 ± 5.7, 27.0 ± 3.2 and 17.6 ± 6.1 °C, respectively, at Site 1 and 20.0 ± 4.8, 28.0 ± 3.4 and 19.0 ± 6.4 °C, respectively, at Site 2. Summary soil nutrient data are presented in Table S3 available as Supplementary Data at *Tree Physiology* Online, and continuous soil moisture and PAR (in the understory) data are presented in Figure S1 available as Supplementary Data at *Tree Physiology* Online.

Gas exchange

Approximately 10,000 observations (945 full or partial curves) were taken from 30 April to 23 October (Julian days 121–297). Observed light saturated assimilation rates showed large variability from low near 0 µmol m^{-2} s^{-1} to maximum rates of around 10 µmol m^{-2} s^{-1} depending on species. Assimilation rates at 400 ppm varied by approximately an order of magnitude or more for each species, with extreme maximum observed rates between 13 and 20 µmol m^{-2} s^{-1} at or above C_i of 1000 ppm depending upon the species (Figure 1).

Model fits and parameter estimates

The final model fits (R^2 between predicted vs observed) were 0.85 for *A. saccharum*, 0.83 for *C. glabra*, 0.84 for *Q. rubra* and 0.80 for *Q. velutina*. Parameter estimates, associated 95% credible intervals and posterior variances for all model parameters are given in Table S4 available as Supplementary Data at *Tree Physiology* Online.

Posterior means and 95% confidence intervals for $\mu g_m 25$, $\mu R_d 25$, $\mu V_{cmax} 25$ and $\mu J_{max} 25$ are presented in Figure 2. Significance can be assessed by comparing 95% confidence intervals, and groups that do not overlap are significantly different ($P < 0.05$). All species except *A. saccharum* showed peak temperature-adjusted mesophyll conductance ($\mu g_m 25$) in summer, and significantly higher rates of temperature-adjusted dark respiration ($\mu R_d 25$) in spring compared with summer and fall (Figure 2a and b). *Quercus velutina* had the highest $\mu g_m 25$ and $\mu R_d 25$ of the four species. *Quercus rubra* also had significantly higher $\mu R_d 25$ in fall than in summer. There were few significant differences in the temperature-adjusted maximum carboxylation rates at mean soil moisture and VPD ($\mu V_{cmax} 25$)
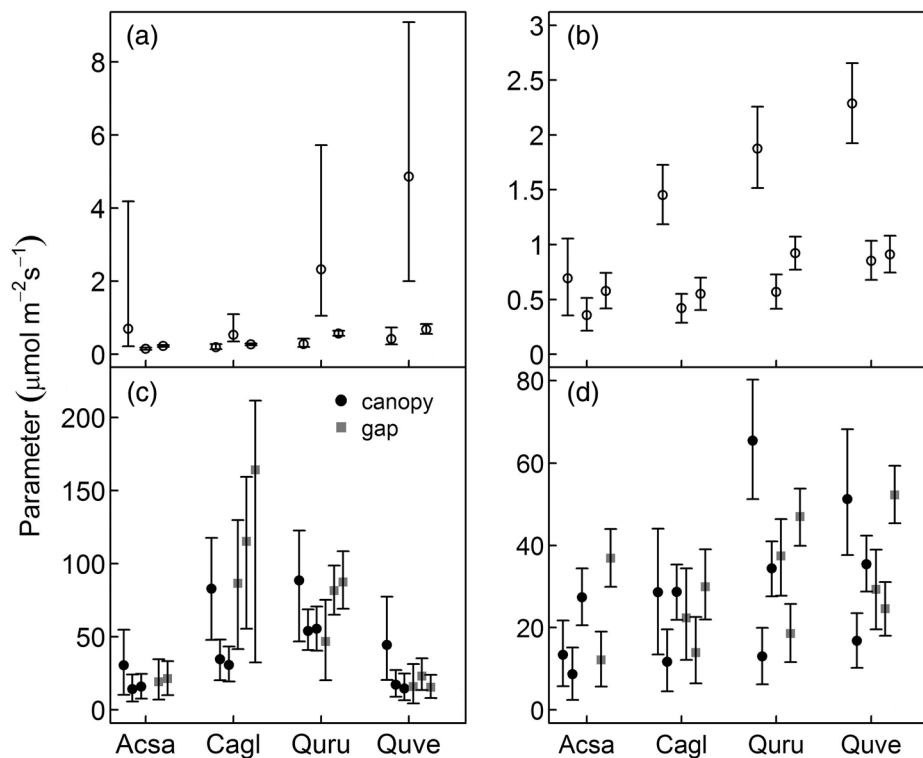
Figure 2. Posterior parameter estimates (and 95% CI) of the main photosynthetic parameters: (a) mesophyll conductance ($\mu g_m 25$), (b) dark respiration ($\mu R_d 25$), (c) maximum Rubisco carboxylation rate ($\mu V_{cmax} 25$) and (d) maximum electron transport rate ($\mu J_{max} 25$) adjusted to 25 °C for canopy (black) and gap (grey) habitats. Estimates vary by season and in some cases also by habitat according to model structure (see 'Materials and methods'). Parameters whose 95% confidence intervals do not overlap are significantly different. Acsa: *A. saccharum*, Cagl: *C. glabra*, Quru: *Q. rubra* and Quve: *Q. velutina*. Note that spring $\mu V_{cmax} 25$ and $\mu J_{max} 25$ estimates for *A. saccharum* are not present as we did not have any gap seedlings in this season.

(Figure 2c). Seedlings of certain species seemed to respond differently to seasonality depending upon light habitats, with higher summer and fall rates in gaps, and higher spring rates in canopy habitats. *Carya glabra* had the highest $\mu V_{cmax}25$ value of the four species and *A. saccharum* had the lowest. The temperature-adjusted maximum electron transport rate at mean soil moisture and VPD ($\mu J_{max}25$) showed more significant differences and tended to be the lowest in summer, regardless of light habitat, particularly for the two *Quercus* species (Figure 2d). $\mu J_{max}25$ was higher in fall than in summer for all four species in both light habitats (the difference in gaps for *C. glabra* was only marginally significant). Significant differences between light habitats depended on the season, with canopy seedlings having higher rates than gap seedlings in spring and lower rates than gap seedlings in fall, particularly for the two *Quercus* spp., but not for *C. glabra*.

In total, three of 20 $\beta 1_{season}$ (effect of soil moisture, allowed to vary by season) and $\beta 2_{habitat}$ (effect of VPD, allowed to vary by light habitat) parameters related to V_{cmax} and 15 of 20 $\beta 1_{season}$ and $\beta 2_{habitat}$ parameters related to J_{max} were significant ($P < 0.05$) (Table S4 available as Supplementary Data at *Tree Physiology* Online reports mean estimates and associated 95% credible intervals). The effect of standardized soil moisture ($\beta 1_{season}$) on V_{cmax} was positive and significant only in summer for *C. glabra* and *Q. rubra*. Standardized VPD ($\beta 2_{habitat}$) had no effect on V_{cmax} except for *A. saccharum* in canopy plots. The effect of soil moisture ($\beta 1_{season}$) on J_{max} varied by season and species. $\beta 1_{season}$ for J_{max} was significant for all seasons in *A. saccharum*, for summer

and fall in *C. glabra*, for spring and summer in *Q. rubra* and only for spring in *Q. velutina*. J_{max} also decreased in summer with soil moisture for *Q. velutina* (marginally significant). J_{max} of *Q. rubra* and *Q. velutina* decreased with increasing soil moisture in spring but increased with soil moisture in summer, while J_{max} for *A. saccharum* and *C. glabra* increased with soil moisture in spring but decreased with soil moisture in summer. J_{max} increased with soil moisture in fall for *A. saccharum* and *C. glabra*. The effect of VPD on J_{max} ($\beta 2_{habitat}$) was uniformly negative across all species and light habitats. $\beta 2_{habitat}$ for J_{max} was significantly more negative in gap plots than in canopy plots for both *A. saccharum* and *C. glabra* seedlings.

Predicted effects of temperature on net assimilation rates

Predictions of net assimilation rates at mean temperature showed no significant differences between seasons or light habitats for any of the four species (Figure 3) ($P > 0.05$). In general, there was wide variability around each of the predictions, and the mean values were quite low, between 1.92 ± 0.99 µmol m^{-2} s^{-1} for canopy plot *A. saccharum* seedlings in summer up to 6.28 ± 1.56 µmol m^{-2} s^{-1} for gap plot *Q. velutina* seedlings in the fall. Predictions of mean assimilation rates tended to be slightly higher in gap habitats than in canopy habitats, but this was not always the case. There were also no significant differences between any assimilation rates among species at mean temperature, though *Quercus* spp. tended to have higher means, and high upper 95% credible interval limits (Figure 3).
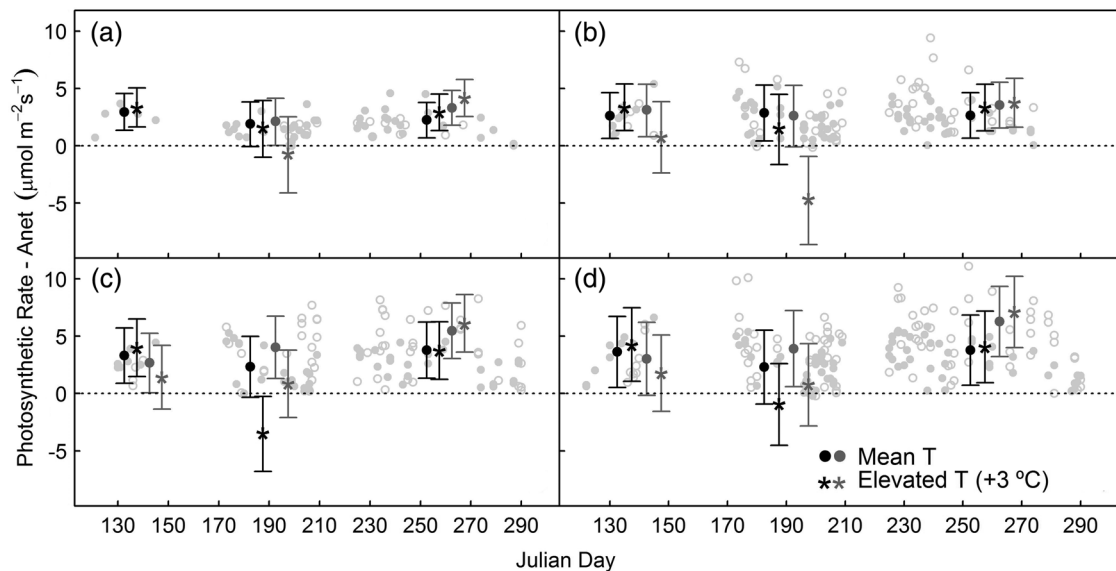
Figure 3. Large points show predictions of net assimilation rates (A_{net}) and 95% CI at mean and elevated (+3 °C) temperatures for each season for (a) *A. saccharum*, (b) *C. glabra*, (c) *Q. rubra* and (d) *Q. velutina*. Negative assimilation rates indicate higher dark respiration than photosynthesis. Colors indicate light habitats and shapes indicate the temperature scenario. Means whose 95% confidence intervals do not overlap are significantly different. Note that spring predictions for *A. saccharum* are not present as we did not have any gap seedlings in this season. Smaller light gray points show time-series of raw light curve data at light levels near those used in predictions (250 for understory and 1000 µmol m^{-2} s^{-1} for gap) for understory (filled light gray circles) and gap (unfilled light gray circles).

The response of predicted assimilation rates to elevated temperatures (Figure 3) varied by season, light habitat and species, though with one exception, there were no significant differences between mean and elevated temperature assimilation rates. In canopy habitats during the summer, *Quercus* spp. seedlings had predicted assimilation rates at elevated temperatures that were much lower than those predicted at current mean temperatures (marginally significant for *Q. rubra*). In gaps in summer, all species tended to have lower predicted assimilation rates at elevated temperatures (significant for *C. glabra*, $P < 0.05$). In general for these three species, the effect of elevated temperature was stronger in summer than in either spring or fall, and negative, while temperature had small positive effects in fall. This pattern was weaker in *A. saccharum*. The ETP quantifies the differences seen in predicted assimilation rates (Table 2). Therefore patterns in ETP mirror those seen in predicted assimilation rates and represent a measure of effect size. The lowest observed ETP was 0.0002, and the highest was 1.70.

Discussion

To better understand how different northeastern North American tree species may respond to climate change, we investigated the effects of environmental variables (soil moisture, VPD, light habitat and temperature) and seasons on seedling carbon assimilation, as this, among other processes, will influence seedling competitive ability. We present evidence that across the species we studied photosynthetic parameters (V_{cmax}, J_{max}, R_d and g_m) vary seasonally. Though environmental variables and seasons are not completely independent, variability in respiration (R_d) and mesophyll conductance (g_m) seems to be independent of environmental variables, while maximum photosynthetic electron transport (J_{max}) and carboxylase activity (V_{cmax}) change with soil moisture and light habitat. Assimilation rates are quite variable in any given season and light habitat. Though mean precipitation is projected to increase (IPCC 2013), increased temperature may still reduce water availability (via increased evapotranspiration), which our results show could restrict the carbon assimilation rates of tree seedlings. Increasing summer temperatures

are predicted to impact seedlings negatively, with >90% decreases in probabilities of achieving current mean assimilation rates in some cases. Conversely, warmer conditions may increase photosynthetic rates in the spring and fall depending on light habitat, potentially compensating for reduced assimilation during the summer, as these seasons may become longer (Menzel and Fabian 1999). However, our measurements do not take into account any potential acclimation to higher temperatures (Tjoelker et al. 1999, Gunderson et al. 2000, Rodríguez-Calcerrada et al. 2010), so although the reported trends are likely to take place, their magnitudes could vary. In summary, our results provide evidence that the effects of future climate change are quite complex, as the response of seedlings' photosynthesis will depend on light habitat and species, and will vary across the growing season.

Q1: Seasonality of dark respiration and mesophyll conductance

The observed peak dark respiration (R_d) in spring (Figure 2) likely corresponds with construction respiration as seedlings build new leaves from stored carbohydrates, and is consistent with some studies (e.g., Zhu et al. 2011; but see Koniger et al. 2000). We measured expanding leaves in the early part of spring for all species. The rise in fall may correspond with bud set (McKown et al. 2013) and dismantling leaf proteins at senescence (Friedrich and Huffaker 1980, Stoddart 1982). Low spring respiration in *A. saccharum* may simply be due to the fact that seedlings of this species were the first to leaf out in spring, perhaps 10 days to 2 weeks prior to sampling, and we may not have begun gas exchange measurements early enough to observe growth respiration. However, as R_d has been shown to acclimate to sustained changes in temperature (Rodríguez-Calcerrada et al. 2010) and we modeled temperature sensitivity of R_d as a single species-level linear response (see 'Analysis'), the observed trend in *C. glabra* and *Quercus* spp. is consistent with temperature acclimation (Tjoelker et al. 1999, Gunderson et al. 2000, Lee et al. 2005), with the highest temperature-adjusted rates in spring and the lowest rates in summer (when temperatures were highest). Possibly it reflects a combination of these two effects.

Table 2. Effect of temperature on photosynthesis, estimated as the change in probability of reaching average current photosynthetic rates while under a climate scenario where the seasonal mean temperature increases by 3 °C. An ETP > 1 indicates an increase in the probability of reaching the current rates and thus a positive effect of a warmer environment, while an ETP < 1 indicates a decrease in the probability of reaching the current rates and thus a negative effect of a warmer environment. Effects were estimated for the two light habitats, understory and gap.

ETP/% change	Spring		Summer		Fall	
Species	Understory (%)	Gap (%)	Understory (%)	Gap (%)	Understory (%)	Gap (%)
A. saccharum	1.35/+35	NA/NA	0.80/−20	0.10/−90	1.60/+60	1.70/+70
C. glabra	1.52/+52	0.15/−85	0.39/−61	0.0002/−99.98	1.49/+49	1.15/+15
Q. rubra	1.39/+39	0.37/−63	0.001/−99.9	0.035/−96.5	0.98/−2	1.38/+38
Q. velutina	1.29/+29	0.46/−52	0.08/−92	0.09/−91	1.13/+13	1.40/+40

Peak mesophyll conductance (g_m) in summer (Figure 2) is likely a function of leaf photosynthetic capacity, with conductance limitation decreasing as leaf expansion and development occur in spring, and then increasing as leaves gradually accrue more damage in fall and senesce. This pattern agrees with the results of certain studies (Grassi and Magnani 2005; but see Zhu et al. 2011). It is unclear why *A. saccharum* did not show the same pattern as the other species, but this species has low drought tolerance (Barnes and Wagner 2004), and the observed pattern may be the result of inhibition or leaf desiccation during the most severe dry period in mid-summer. Drought has been shown to negatively impact g_m (Keenan et al. 2010, Cano et al. 2013). Methods that explicitly assess mesophyll conductance (e.g., fluorescence measurements) are likely required to assess seasonality in this parameter, as it was difficult to reliably identify without restrictive priors (see 'Prior distributions', Table 1).

Q1: Seasonality of V_{cmax} and J_{max}

The maximum carboxylation rate (V_{cmax}) and the maximum electron transport rate (J_{max}) are two commonly estimated photosynthetic parameters, as they represent two important biochemical limitations to carbon assimilation encountered under natural conditions. Studies have shown that V_{cmax} and J_{max} peak in mid-summer in temperate trees (Bauerle et al. 2012, Stoy et al. 2014). While we were estimating J_{max} and V_{cmax} at mean soil moisture and VPD, we did not observe a mid-summer peak in these parameters (Figure 2). This discrepancy is likely due to the fact that we studied seedlings, which are more vulnerable to environmental fluctuations than adult trees (Zhu et al. 2011, Stoy et al. 2014) or saplings (Bauerle et al. 2012).

There were large differences in mean VPD, soil moisture and temperature between canopy and gap habitats, as well as differences in incident light levels (data not shown), likely causing the effects of mid-summer drought to vary in severity by light habitat. Compared with a mid-season peak, our result of minimum J_{max} during the summer in gaps, and no mid-summer peak in V_{cmax}, suggests drought inhibition (Figure 2). Differences in phenology between canopy and gap seedlings may complicate the interpretation of these results; however, this pattern likely indicates that important summer carbon gains may be lost under increased temperature and aridity in this system.

Q2: Effects of environmental variables: interactions with seasonality

While the effects of light habitat on V_{cmax} and J_{max} vary by season, increased values of J_{max} in *Quercus* spp. and higher V_{cmax} in *C. glabra* and *Q. rubra* in gaps following larger and more frequent rain events in the fall suggest that typical acclimation to the light environment was masked earlier in the season by dry conditions (Figure 2, Figure S1 available as Supplementary

Data at *Tree Physiology* Online). Though we did not measure leaf nitrogen or whole-plant leaf area, plants in gaps typically invest less nitrogen in expensive leaf proteins (chlorophyll and thylakoid proteins) for light capture and instead maintain higher electron transport efficiency per unit chlorophyll (Evans 1989, Evans and Poorter 2001). Lower J_{max} in spring in gaps may be due to slower development of photosynthetic capacity in gap seedlings, which leafed out ~2 weeks later than canopy seedlings for all species. Unfortunately, it is difficult to isolate the effects of drought and season when assessing the response of seedling assimilation to light habitat, as summer was the driest season.

The large number of significant parameters related to J_{max}, particularly for VPD, may indicate that variation in J_{max} is not fully explained by the C_i data, and that drought-induced decreases in J_{max} may have been due in part to non-stomatal effects (Table S4 available as Supplementary Data at *Tree Physiology* Online). Moderately low leaf water potential may directly limit the rates of RUBP regeneration (Kaiser 1987) as well as Rubisco carboxylation (Maroco et al. 2002). It is also possible that at high VPD or at low assimilation rates, the C_i estimated by the LI-6400 is less accurate (Kaiser 1987). A third possibility is that low J_{max} at high VPD may be primarily due to decreases in mesophyll conductance, as decreases in V_{cmax} and J_{max} may only be responsible for significant limitation during severe dry conditions (e.g., Grassi and Magnani 2005). Due to the model structure, and our difficulty in reliably identifying g_m, we are unable to differentiate between these cases. However, regardless of whether this represents non-stomatal effects or C_i measurement errors, utilization of VPD and soil moisture data improves the estimation of J_{max}, without the need to incorporate a computationally intensive stomatal conductance model.

Q3: Predicted assimilation rates under future climate

Predictions suggest that high temperatures, low soil moistures and high VPDs due to drought minimize absolute differences in net assimilation rates among species, while the predicted variability around photosynthetic rates is large (Figure 3). Predictions also show that *Quercus* spp. (particularly *Q. velutina*) may be better competitors than the other species due to their higher potential assimilation rates across seasons and habitats, though they generally perform better in gaps (Figure 3). While we did not estimate seedling carbon balances, our repeated measures of instantaneous gas exchange rates on multiple seedlings over an entire growing season, resulting in a much larger sample size than comparable studies (e.g., Kwit et al. 2010), provide ample information about the potential competitive differences between species (e.g., Rebbeck et al. 2012). Thus while we do not have the resolution to estimate individual carbon budgets for the study of seedlings, the extent of our data and model specificity (replication of individuals and

light habitats, seasonal and daily measurements, and a model that accurately quantifies population variability around mean rates) allow us to make inferences about the relative competitive abilities of these species. Differences in rates, compounded over multiple years, may lead to large differences in resource acquisition and growth (Monteith 1965, Noland et al. 1996, Kirschbaum 2011), indicating that *Quercus* spp. may be competitively favored under future climate conditions over *A. saccharum*, and even *C. glabra* in the seedling stage.

Results of elevated temperature predictions indicate important differences in performance at warmer temperatures. The effect of higher temperature (+3 °C) on photosynthesis (ETP) in summer indicates strong negative effects on photosynthesis for all species, regardless of light habitat (Table 2). Particularly in gaps, seedlings of all four species will be unable to achieve current assimilation rates under elevated temperatures. Strong negative effects were also found in spring in gaps and in summer in the understory (Table 2). Thus, seedlings' survival in gap habitats could be negatively impacted, further narrowing the recruitment potential for these species. Conversely, smaller increases in the ETP in spring and fall, particularly in the understory, coupled with future increases in growing season length may lessen these impacts somewhat, as seedlings make up for summer losses during more favorable spring and fall conditions. However, these results do not take into account any potential acclimation of the seedlings to higher temperature.

In particular, R_d has been shown to acclimate to sustained changes in temperature (Gunderson et al. 2000, Tjoelker et al. 2001, Lee et al. 2005, Rodríguez-Calcerrada et al. 2010, but see Dillaway and Kruger 2011 and references therein). While we do not directly account for this effect in our ETP predictions, we allow $\mu R_d 25$ to vary seasonally, which partially captures the effects of progressive acclimation to higher temperatures between seasons. However, this means we likely overestimate increases in dark respiration in our elevated temperature predictions. Most studies of respiration temperature acclimation compare acclimated seedlings at a reference temperature. Of those which give full temperature response curves of seedlings acclimated to different temperatures, some species alter temperature responses to maintain a relatively equal R_d at different temperatures (for a potential ~13% overestimate ignoring acclimation for *A. saccharum* [estimated from Gunderson et al. 2000]) while more responsive species show smaller increases than would be predicted assuming no acclimation. We were unable to find comparable data for the other three species. An upper limit of the overestimate for North American temperate deciduous species seems to be ~25% for *Betula papyrifera* Marsh. and *Populus tremuloides* Michx. (estimated from Tjoelker et al. 1999).

Furthermore, photosynthesis itself may not acclimate to increases in temperature (Liang et al. 2013), and reports of acclimation in R_d are not universal for these species (e.g., Wertin et al. 2011) or other North American deciduous

species, and mechanisms are still not completely understood (Dillaway and Kruger 2011). Vapor pressure deficit increases were also included in the predictions, and as the effect of VPD on J_{max} (representing both stomatal and non-stomatal effects) was always negative, this variable played a significant role in the predicted ETP responses. While stomatal conductance may acclimate to increased temperature at constant VPD (Santrucek and Sage 1996), it is unlikely that conductance acclimates to changes in VPD, and the mechanism for such a response is unclear. Non-stomatal components of ETP response represent the damage to photosynthetic machinery or cell structure (Yordanov et al. 2000, Flexas and Medrano 2002) or down-regulation (Chaves et al. 2009). Therefore, the exclusion of explicit temperature acclimation of R_d from our model does not invalidate our ETP predictions, though decreases in ETP are likely somewhat overestimated. Plants exhibit higher water water-use efficiency at elevated CO_2 concentrations (Kimball et al. 1993, Drake et al. 1997, De Kauwe et al. 2013), which may lessen the magnitude of responses under future climate conditions, but this is beyond the scope of this study.

Conclusion

Based on our results, the net impact over a growing season will determine species' ability to assimilate carbon. Our predictions show that seedling phostosynthetic rates may be strongly impacted by climate change-induced warming, but this will depend on the light habitat and the specific day during the growing season, as key photosynthetic parameters vary seasonally. While many other factors play into competitive ability and demographics, these changes are likely to have significant effects on seedling recruitment through time as small differences in rates compound over multiple years. While all species are likely to respond negatively, the combined impacts of increased VPD and temperature seem to favor *Quercus* spp. seedlings over *A. saccharum* and *C. glabra* seedlings. Increased oak species dominance and *A. saccharum* decline under forecasted climate have been predicted by several species distribution models for the region (Prasad et al. 2007, Iverson et al. 2008), but hickory species, in particular *C. glabra*, are also predicted to increase in abundance as temperatures rise and temperate forests become more arid. Though long-term population demographics will also depend on processes at other life stages, these results suggest that changes in recruitment patterns of these species in the region may take place under projected climate change, particularly as warmer years and droughts become more common.

Authors' contributions

D.M.P.P. and I.I. conceived the experiment. D.M.P.P. formulated methodology, conducted fieldwork, implemented the model and performed the analysis. D.M.P.P. and I.I. wrote the manuscript.

Supplementary data

Acknowledgments

Conflict of interest

All experiments performed comply with the current laws of the USA.

Funding

References

Allen CD, Macalady AK, Chenchouni H et al. (2010) A global overview of drought and heat-induced tree mortality reveals emerging climate change risks for forests. For Ecol Manag 259:660–684.

Andresen J (2012) Michigan Drought Update for July 12, 2012. Michigan State University Extension. http://msue.anr.msu.edu/news/michigan_drought_update_for_july_12_2012 (12 February 2014, date last accessed).

Aranda I, Castro L, Pardos M, Gil L, Pardos JA (2005) Effects of the interaction between drought and shade on water relations, gas exchange and morphological traits in cork oak (*Quercus suber* L.) seedlings. For Ecol Manag 210:117–129.

Augspurger CK, Cheeseman JM, Salk CF (2005) Light gains and physiological capacity of understorey woody plants during phenological avoidance of canopy shade. Funct Ecol 19:537–546.

Barnes BV, Wagner WH Jr (2004) Michigan trees. University of Michigan Press, Ann Arbor, MI.

Bauerle WL, Oren R, Way DA et al. (2012) Photoperiodic regulation of the seasonal pattern of photosynthetic capacity and the implications for carbon cycling. Proc Natl Acad Sci USA 109:8612–8617.

Bethers S, Day ME, Wiersma GB, Fernandez IJ, Elvir JA (2009) Effects of chronically elevated nitrogen and sulfur deposition on sugar maple saplings: nutrition, growth and physiology. For Ecol Manag 258: 895–902.

Björkman O, Powles SB (1984) Inhibition of photosynthetic reactions under water stress: interaction with light level. Planta 161:490–504.

Björkman O, Badger MR, Armond PA (1980) Response and adaptation of photosynthesis to high temperatures. In: Turner NC, Kramer PJ (eds) Adaptation of plants to water and high temperature stress. Wiley, New York, pp 233–249.

Burkholder PR (1936) The role of light in the life of plants. I. Light and physiological processes. Bot Rev 2:1–52.

Caemmerer S (2000) Biochemical models of leaf photosynthesis. Techniques in Plant Sciences, 2. CSIRO Publishing, Collingwood, VIC, Australia.

Caemmerer S, Evans JR (1991) Determination of the average partial pressure of CO_2 in chloroplasts from leaves of several C_3 plants. Funct Plant Biol 18:287–305.

Cano FJ, Sánchez-Gómez D, Rodríguez-Calcerrada J, Warren CR, Gil L, Aranda I (2013) Effects of drought on mesophyll conductance and photosynthetic limitations at different tree canopy layers. Plant Cell Environ 36:1961–1980.

Caspersen JP, Kobe RK (2001) Interspecific variation in sapling mortality in relation to growth and soil moisture. Oikos 92:160–168.

Chaves MM, Flexas J, Pinheiro C (2009) Photosynthesis under drought and salt stress: regulation mechanisms from whole plant to cell. Ann Bot 103:551–560.

Comita LS, Uriarte M, Thompson J, Jonckheere I, Canham CD, Zimmerman JK (2009) Abiotic and biotic drivers of seedling survival in a hurricane-impacted tropical forest. J Ecol 97:1346–1359.

Davies WJ, Mansfield TA, Wellburn AR (1980) A role for abscisic acid in drought endurance and drought avoidance. In: Skoog F (ed) Plant growth substances 1979. Springer, Berlin, Heidelberg, pp 242–253.

DeLucia EH, Thomas RB (2000) Photosynthetic responses to CO_2 enrichment of four hardwood species in a forest understory. Oecologia 122:11–19.

De Kauwe MG, Medlyn BE, Zaehle S et al. (2013) Forest water use and water use efficiency at elevated CO_2: a model-data intercomparison at two contrasting temperate forest FACE sites. Glob Change Biol 19:1759–1779.

De Steven D (1994) Tropical tree seedling dynamics: recruitment patterns and their population consequences for three canopy species in Panama. J Trop Ecol 10:369–383.

Dillaway DN, Kruger EL (2011) Leaf respiratory acclimation to climate: comparisons among boreal and temperate tree species along a latitudinal transect. Tree Physiol 31:1114–1127.

Dillaway DN, Kruger EL (2014) Trends in seedling growth and carbon-use efficiency vary among broadleaf tree species along a latitudinal transect in eastern North America. Glob Change Biol 20:908–922.

Drake BG, Gonzàlez-Meler MA, Long SP (1997) More efficient plants: a consequence of rising atmospheric CO_2? Ann Rev Plant Biol 48:609–639.

Dreyer E, Le Roux X, Montpied P, Daudet FA, Masson F (2001) Temperature response of leaf photosynthetic capacity in seedlings from seven temperate tree species. Tree Physiol 21:223–232.

Dubois JJB, Fiscus EL, Booker FL, Flowers MD, Reid CD (2007) Optimizing the statistical estimation of the parameters of the Farquhar–von Caemmerer–Berry model of photosynthesis. New Phytol 176:402–414.

Evans JR (1987) The relationship between electron transport components and photosynthetic capacity in pea leaves grown at different irradiances. Aust J Plant Physiol 14:157–170.

Evans JR (1989) Photosynthesis and nitrogen relationships in leaves of C_3 plants. Oecologia 78:9–19.

Evans JR, Poorter H (2001) Photosynthetic acclimation of plants to growth irradiance: the relative importance of specific leaf area and nitrogen partitioning in maximizing carbon gain. Plant Cell Environ 24:755–767.

Farquhar GD, Sharkey TD (1982) Stomatal conductance and photosynthesis. Annu Rev Plant Physiol 33:317–345.

Farquhar GD, Wong SC (1984) An empirical model of stomatal conductance. Aust J Plant Physiol 11:191–210.

Farquhar GD, von Caemmerer S, Berry JA (1980) A biochemical model of photosynthetic CO_2 assimilation in leaves of C_3 species. Planta 149:78–90.

Flexas J, Medrano H (2002) Drought-inhibition of photosynthesis in C_3 plants: stomatal and non-stomatal limitations revisited. Ann Bot 89:183–189.

Friedrich JW, Huffaker RC (1980) Photosynthesis, leaf resistances, and ribulose-1,5-bisphosphate carboxylase degradation in senescing barley leaves. Plant Physiol 65:1103–1107.

Garrett ES, Zeger SL (2000) Latent class model diagnosis. Biometrics 56:1055–1067.

Gelman A, Rubin DB (1992) Inference from iterative simulation. Stat Sci 7:457–511.

Grassi G, Magnani F (2005) Stomatal, mesophyll conductance and biochemical limitations to photosynthesis as affected by drought and leaf ontogeny in ash and oak trees. Plant Cell Environ 28:834–849.

Gray AN, Spies TA (1997) Microsite controls on tree seedling establishment in conifer forest canopy gaps. Ecology 78:2458–2473.

Gunderson CA, Norby RJ, Wullschleger SD (2000) Acclimation of photosynthesis and respiration to simulated climatic warming in northern and southern populations of *Acer saccharum*: laboratory and field evidence. Tree Physiol 20:87–96.

Harcombe PA (1987) Tree life tables. Bioscience 37:557–568.

Harper JL (1977) Population biology of plants. London: Academic Press.

Havranek WM, Benecke U (1978) The influence of soil moisture on water potential, transpiration and photosynthesis of conifer seedlings. Plant Soil 49:91–103.

Ibáñez I, McCarthy-Neumann S (2013) Plant–soil feedback links negative distance dependence and light gradient partitioning during seedling establishment. Ecology 94:780–786.

Ibáñez I, Clark JS, Dietze MC (2008) Evaluating the sources of potential migrant species: implications under climate change. Ecol Appl 18:1664–1678.

Ibáñez I, Clark JS, Dietze MC (2009) Estimating performance of potential migrant species. Glob Change Biol 15:1173–1188.

IPCC (2007) The physical science basis. Contribution of working group I to the fourth assessment report of the intergovernmental panel on climate change. Cambridge University Press, Cambridge, UK, New York, NY.

IPCC (2013) Working group I contribution to the IPCC fifth assessment report, climate change 2013: the physical science basis, summary for policymakers. Cambridge University Press, Cambridge, UK, New York, NY.

Iverson LR, Prasad AM, Matthews SN, Peters M (2008) Estimating potential habitat for 134 eastern US tree species under six climate scenarios. For Ecol Manag 254:390–406.

Johnston ES (1940) Sunlight and plant life. Sci Mon 50:513–525.

Kaiser WM (1987) Effects of water deficit on photosynthetic capacity. Physiol Plant 71:142–149.

Keenan T, Sabate S, Gracia C (2010) The importance of mesophyll conductance in regulating forest ecosystem productivity during drought periods. Glob Change Biol 16:1019–1034.

Kimball BA, Mauney JR, Nakayama FS, Idso SB (1993) Effects of increasing atmospheric CO_2 on vegetation. Vegetatio 104:65–75.

Kirschbaum MUF (2011) Does enhanced photosynthesis enhance growth? Lessons learned from CO_2 enrichment studies. Plant Physiol 155:117–124.

Kobe R, Pacala S, Silander J, Canham C (1995) Juvenile tree survivorship as a component of shade tolerance. Ecol Appl 5:517–532.

Koniger M, Harris GC, Kibler E (2000) Seasonal changes in the physiology of shade leaves of *Acer saccharum*. J Plant Physiol 157:627–636.

Kwit MC, Rigg LS, Goldblum D (2010) Sugar maple seedling carbon assimilation at the northern limit of its range: the importance of seasonal light. Can J For Res 40:385–393.

Laube J, Sparks TH, Estrella N, Höfler J, Ankerst DP, Menzel A (2014) Chilling outweighs photoperiod in preventing precocious spring development. Glob Change Biol 20:170–182.

Lee TD, Reich PB, Bolstad PV (2005) Acclimation of leaf respiration to temperature is rapid and related to specific leaf area, soluble sugars and leaf nitrogen across three temperate deciduous tree species. Func Ecol 19:640–647.

Liang J, Xia J, Liu L, Wan S (2013) Global patterns of the responses of leaf-level photosynthesis and respiration in terrestrial plants to experimental warming. J Plant Ecol 6:437–447.

Lunn D, Spiegelhalter D, Thomas A, Best N (2009) The BUGS project: evolution, critique and future directions. Stat Med 28:3049–3067.

Man RZ, Lieffers VJ (1997) Seasonal photosynthetic responses to light and temperature in white spruce (*Picea glauca*) seedlings planted under an aspen (*Populus tremuloides*) canopy and in the open. Tree Physiol 17:437–444.

Maroco JP, Rodrigues ML, Lopes C, Chaves MM (2002) Limitations to leaf photosynthesis in field-grown grapevine under drought—metabolic and modelling approaches. Funct Plant Biol 29:451–459.

Matthes U, Larson DW (2006) Microsite and climatic controls of tree population dynamics: an 18-year study on cliffs. J Ecol 94:402–414.

McKown AD, Guy RD, Azam MS, Drewes EC, Quamme LK (2013) Seasonality and phenology alter functional leaf traits. Oecologia 172:653–665.

Menzel A, Fabian P (1999) Growing season extended in Europe. Nature 397:659–659.

Monteith JL (1965) Light distribution and photosynthesis in field crops. Ann Bot 29:17–37

Mooney HA (1972) The carbon balance of plants. Annu Rev Ecol Syst 3:315–346.

Morin X, Lechowicz MJ, Augspurger C, O'Keefe J, Viner D, Chuine I (2009) Leaf phenology in 22 North American tree species during the 21st century. Glob Change Biol 15:961–975.

Niinemets O, Diaz-Espejo A, Flexas J, Galmes J, Warren CR (2009) Importance of mesophyll diffusion conductance in estimation of plant photosynthesis in the field. J Exp Bot 60:2271–2282.

NOAA National Climatic Data Center (2012) State of the Climate: Drought for June 2012. http://www.ncdc.noaa.gov/sotc/drought/2012/6 (12 March 2014, date last accessed).

Noland TL, Mohammed GH, Scott M (1996) The dependance of root growth potential on light level, photosynthetic rate, and root starch content in jack pine seedlings. New For 13:105–119.

Norton JM, Smith JL, Firestone MK (1990) Carbon flow in the rhizosphere of ponderosa pine seedlings. Soil Biol Biochem 22:449–455.

Oren R, Sperry JS, Katul GG, Pataki DE, Ewers DE, Phillips N, Schäfer KVR (1999) Survey and synthesis of intra- and interspecific variation in stomatal sensitivity to vapour pressure deficit. Plant Cell Environ 22:1515–1526.

Patrick LD, Ogle K, Tissue DT (2009) A hierarchical Bayesian approach for estimation of photosynthetic parameters of C3 plants. Plant Cell Environ 32:1695–1709.

Prasad AM, Iverson LR, Matthews S, Peters M (2007) A climate change atlas for 134 forest tree species of the eastern United States. Northern Research Station, USDA Forest Service, Delaware, OH.

Quero JL, Villar R, Marañón T, Zamora R, Vega D, Sack L (2008) Relating leaf photosynthetic rate to whole plant growth: drought and shade effects on seedlings of four *Quercus* species. Funct Plant Biol 35:725–737.

Rebbeck J, Scherzer A, Gottschalk K (2012) Do chestnut, northern red, and white oak germinant seedlings respond similarly to light treatments? II. Gas exchange and chlorophyll responses. Can J For Res 42:1025–1037.

Rich PM (1990) Characterizing plant canopies with hemispherical photographs. Remote Sens Rev 5: Special issue: instrumentation for studying vegetation canopies for remote sensing in optical and thermal infrared regions, pp 13–29.

Rodríguez-Calcerrada J, Atkin OK, Robson TM, Zaragoza-Castells J, Gil L, Aranda I (2010) Thermal acclimation of leaf dark respiration of

beech seedlings experiencing summer drought in high and low light environments. Tree Physiol 30:214–224.

Santrucek J, Sage RF (1996) Acclimation of stomatal conductance to a CO_2-enriched atmosphere and elevated temperature in *Chenopodium album*. Funct Plant Biol 23:467–478.

Schneider CA, Rasband WS, Eliceiri KW (2012) NIH image to ImageJ: 25 years of image analysis. Nat Methods 9:671–675.

Sharkey TD, Imai K, Farquhar GD, Cowan IR (1982) A direct confirmation of the standard method of estimating intercellular partial pressure of CO_2. Plant Physiol 69:657–659.

Stoddart TH (1982) Leaf senescence. In: Boulter D, Parthier B (eds) Nucleic acids and proteins in plants I (Encyclopedia of plant physiology), Vol. 14. Springer, Berlin, Heidelberg, New York, pp 592–636.

Stoy PC, Trowbridge AM, Bauerle WL (2014) Controls on seasonal patterns of maximum ecosystem carbon uptake and canopy-scale photosynthetic light response: contributions from both temperature and photoperiod. Photosynth Res 119:49–64.

Tezara W, Mitchell VJ, Driscoll SD, Lawlor DW (1999) Water stress inhibits plant photosynthesis by decreasing coupling factor and ATP. Nature 401:914–917.

Tjoelker MG, Reich PB, Oleksyn J (1999) Changes in leaf nitrogen and carbohydrates underlie temperature and CO_2 acclimation of dark respiration in five boreal tree species. Plant Cell Environ 22:767–778.

Tjoelker MG, Oleksyn J, Reich PB (2001) Modelling respiration of vegetation: evidence for a general temperature-dependent Q10. Glob Change Biol 7:223–230.

Wertin TM, McGuire MA, Teskey RO (2011) Higher growth temperatures decreased net carbon assimilation and biomass accumulation of northern red oak seedlings near the southern limit of the species range. Tree Physiol 31:1277–1288.

Wilson KB, Baldocchi DD, Hanson PJ (2000) Spatial and seasonal variability of photosynthetic parameters and their relationship to leaf nitrogen in a deciduous forest. Tree Physiol 20:565–578.

Yordanov I, Velikova V, Tsonev T (2000) Plant responses to drought, acclimation, and stress tolerance. Photosynthetica 38:171–186.

Zhu GF, Li X, Su YH, Lu L, Huang CL (2011) Seasonal fluctuations and temperature dependence in photosynthetic parameters and stomatal conductance at the leaf-scale of *Populus euphratica* oliv. Tree Physiol 31:178–195.